JMEPEG (2001) 10:484–492

Graphitization of Steels in Elevated-Temperature Service

J.R. Foulds and R. Viswanathan

(Submitted 17 May 2000)

Prolonged exposure of carbon and low alloy steel components to temperatures exceeding 800 °F (427 °C) can result in several kinds of material microstructural deterioration; for example, creep cavitation, carbide coarsening and/or spheroidization, and, less commonly, graphitization. Graphitization generally results from the decomposition of pearlite (iron + iron carbide) into the equilibrium structure of iron + graphite and can severely embrittle the steel when the graphite particles or nodules form in a planar, continuous manner. Graphitization has resulted in the premature failure of pressure boundary components, including high energy piping and boiler tubes. Failure due to graphitization continues to be of concern in long-term aged carbon and carbon-molybdenum steels, both in weldments and in base metal, where, as recently reported, prior deformation or cold work could accelerate the graphitization process. This paper describes the characteristics and kinetics of graphitization, reviews pertinent laboratory and field experience, and summarizes time-temperature service regimes within which graphitization can be anticipated.

Introduction and Background

Graphitization may be defined, in general, as the formation of free carbon, C (graphite), in iron or steel. Graphite formed during the solidification process is called primary graphitization, resulting in the stable iron-graphite structure. Gray (flake graphite) iron, ductile (spheroidal graphite) iron, and compacted graphite iron are cast irons representing examples of a primary graphitization product. Graphite formation through the transformation of metastable metallic carbides following solidification is termed secondary graphitization. The most common process of secondary graphitization involves the decomposition of pearlite (iron + iron carbide) by transformation of the iron carbide, Fe_3C (cementite), at elevated temperature, to iron and graphite. The age-related graphitization of carbon and low alloy steel in elevated-temperature fossil plant (or other) service is an example of secondary graphitization. In comparison with graphitization that may be intentional or expected, as in the case of cast irons, the in-service phenomenon in carbon and low alloy steels is unintentional and sometimes results in material property changes that are detrimental to the integrity of the operating component.

It is generally known that carbide spheroidization competes with graphitization in carbon and low alloy steels subject to elevated-temperature service. Which one of the two processes (graphitization or spheroidization) occurs depends on the steel composition and microstructure and on the exposure temperature. Increasing temperatures favor spheroidization. The *Metals Handbook*[1] shows, as an example, the temperature regimes within which either spheroidization (above 1025 °F or 552 °C) or graphitization (below 1025 °F or 552°C) can be expected to be the dominant transformation process. In reality, field experience indicates (*e.g.*, Ref 2) that the graphitization-to-spheroidization transition temperature varies in a manner not entirely predictable and, in a particular instance, may differ significantly from the 1025 °F (552 °C) value suggested by the example of Ref 1. Due to its potential embrittling effect, graphitization is of greater concern than is spheroidization. Therefore, an initial conservative prediction of graphitization may be made by assuming that spheroidization does not occur. The conservatism can be subsequently reduced by implementation of a component-specific inspection program based on the prediction.

J.R. Foulds, Exponent Failure Analysis Associates, Inc., Menlo Park, CA; and **R. Viswanathan,** Electric Power Research Institute, Palo Alto, CA.

This paper was originally printed as part of a TMS Proceedings, *Graphitization of Steels in Elevated-Temperature Service,* proceedings, First International Conference on Microstructures and Mechanical Properties of Aging Materials, P.K. Liaw et al., ed., The Minerals, Metals and Materials Society, Warrendale, PA, 1993, pp. 61–69.

In-Service Failures and Related Research

In 1943, a carbon-molybdenum (C-Mo) steel steam pipe at the Springdale Power Station of the West Penn Power Company ruptured catastrophically at a girth weld.[3] The pipe had been in service for 5-1/2 years at a temperature of 935 °F (502 °C) and was found to have ruptured along a "plane of graphite" running through the wall and parallel to the girth weld in the low-temperature region of the weld heat-affected zone (HAZ). This failure provided the initial motivation for investigation into the phenomenon of in-service graphitization of pressure boundary, elevated-temperature, carbon and low alloy steel components in both the power generation and process industries. Early studies[4,5] shortly following the Springdale failure resulted in some general conclusions on the effect of steel chemistry and exposure temperature on the susceptibility to graphitization. The adverse effects of aluminum (Al) and silicon (Si) and the beneficial effect of chromium (Cr) on graphitization resistance were reported. Further, it was concluded that weld HAZ graphitization of C-Mo steel piping could be avoided with control of exposure temperature to below 800 °F (427 °C).

Despite careful application of this knowledge regarding graphitization to operating power plant piping, the Oak Ridge Gaseous Diffusion Plant experienced, in 1957, two major power plant component failures due to graphitization.[6] These failures occurred due to graphitization of a form similar to the Springdale case and were in the weld HAZs of C-Mo main steam piping that had been in service for >100,000 h at 935 °F (502 °C) design conditions. The Oak Ridge experience showed the considerable predictive uncertainty associated with graphitization, since the prior implementation of a relatively extensive sampling program had proved ineffective in preventing the graphitization failures.

Following the Oak Ridge failures and based on graphitization research conducted in the 1940s, 1950s, and 1960s, including the American Petroleum Institute (API) sponsored effort to assess the graphitized condition and estimate future graphitization of pertinent operating refinery equipment,[7] it was generally concluded that carbon (C) and C-Mo steels were susceptible to graphitization when exposed to service temperatures exceeding 800 °F (427 °C) and that the addition of Cr to these steels in an amount exceeding 0.5% would permit extended, graphite-free operation above 800 °F (427 °C). Further, it became widely accepted that weld-unaffected C and C-Mo steel base metal was unlikely to suffer the severe planar form of graphitization that had caused the previous failures.

Thus, material changes from C and C-Mo steel to CrMo steels, and cautious operation and maintenance of existing C and C-Mo steel components, reduced the level of concern and subsequent research into the phenomenon of in-service graphitization. Even so, a serious graphitization-related failure again occurred in 1977 at Pennelec's Williamsburg Station.[8] Following this failure, there have been several less severe, yet unexpected cases of graphitization in C and C-Mo steel components.[9–11] These more recent observations have been surprising since they include the occurrence of a planar form of graphitization in base metal, unrelated to any welds. The planar graphite morphology in base metal has the potential of producing failures of the catastrophic magnitude of the Springdale case and merits the concern given the weld-related problem.

Forms of Graphitization

Graphitization in the form of randomly dispersed nodules is relatively benign. This form of graphitization has been observed in carbon and low alloy steel weldments and base metal and is not of major concern since it does not cause serious embrittlement. However, the formation of a chain or "plane" of graphite by localized nucleation and growth of such nodules can result in a significant reduction in the load-bearing capacity of the component with an increased potential for catastrophic, brittle fracture along this plane. Two basic forms of chain, or planar graphitization, may be defined on the basis of location relative to weld metal. These forms are categorized as "weld HAZ graphitization" and "base metal graphitization."

Weld HAZ Graphitization. This form of graphitization has been responsible for the earlier catastrophic failures (*e.g.*, Refs 3 and 6) described above, and has been relatively well-researched. Graphitization in this case occurs in the HAZ of a weld in carbon or low alloy steel along a plane parallel to, and at some distance from, the weld-base metal interface. The approximately constant distance from the interface is largely determined by the peak temperature during the weld thermal cycle (temperature slightly above the lower-critical temperature, Ac_1), which results in a supersaturation of carbon at this location, driving graphite nucleation, and growth. In a cross section normal to the weld direction, the plane of graphite appears as a line parallel to the weld-base metal interface, giving the appearance of "eyebrows," hence, the term "eyebrow graphitization." Figure 1 is a macrograph showing an example of this form of graphitization in a carbon steel weldment.

Base Metal Graphitization. Recent observations of graphitization include a "new" form of graphitization in base metal unrelated to welding. This new form, also called "non-weld-related graphitization," merits as much concern as the weld HAZ graphitization causing the early catastrophic failures because it also occurs in a chainlike manner. It has been concluded that this form of graphitization occurs in regions believed to have experienced significant plastic deformation.[10,11] Figure 2 is a macroscopic cross-section view of a C-Mo steel boiler tube that has experienced this form of graphitization, resulting in tube rupture. The apparent "graphitized" lines represent graphitized planes believed to be coincident with deformation bands resulting from plastic strain.[10,11]

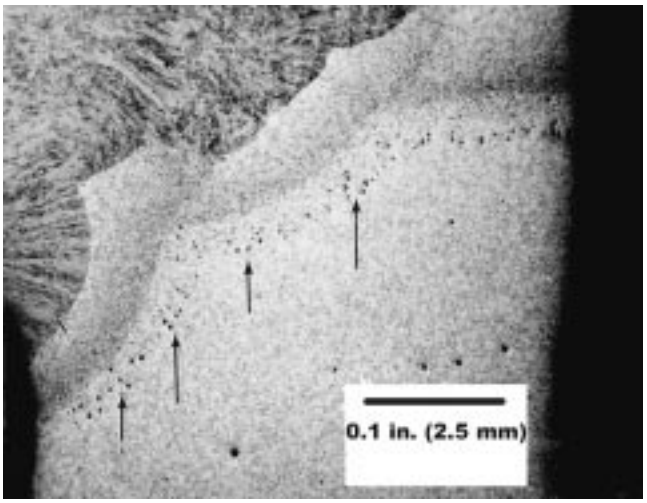

Fig. 1 Macrograph of an ex-service C steel weldment exhibiting weld HAZ graphitization

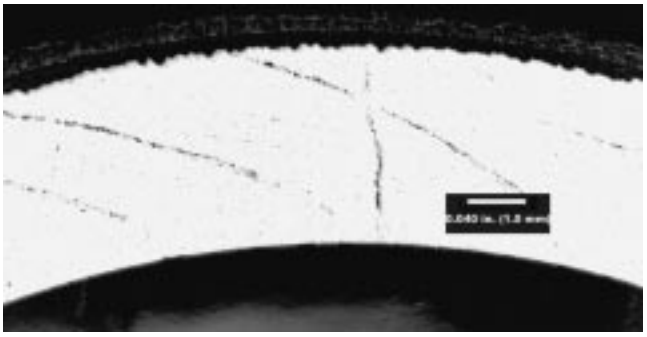

Fig. 2 Macrograph of the cross section of a portion of a failed C-Mo boiler tube showing non-weld-related graphitization (photograph courtesy of R. Hellner, Public Service Co. of Colorado)

Graphite Formation

Graphite formation in C, C-Si, and C-Mo steels during elevated-temperature service occurs mainly as a result of the transformation of the metastable cementite into iron and graphite:

$$Fe_3C \Rightarrow 3Fe + C$$

The process details, however, include both a graphite nucleation and a subsequent growth phase. Graphite nucleation is

primarily driven by the availability of appropriate nucleation sites, while the graphite growth kinetics are generally controlled by the diffusion/transport of the slowest moving species resulting in free carbon at the nucleated, existing graphite phase. The nucleation, growth, and morphology of graphite, and conditions under which graphitization may be avoided (derived from published field and laboratory data), are discussed in the following.

Graphite Nucleation

Two factors influence the susceptibility to graphite nucleation: the existence of an appropriate nucleation site and the generation/availability of free carbon to produce the critical nucleus size. It is generally accepted that graphite nucleation in iron and steel occurs in a heterogeneous fashion at sites where free carbon can be produced or to which free carbon can be effectively transported, and where the volume and graphite-matrix interface changes in subcritical nucleus growth can be accommodated. Baranov and Bunin[12] demonstrated this nearly 30 years ago, by theory and experiment. Since the critical graphite nucleus size is probably submicroscopic (reported to be as low as 4.1 Å by one investigator[13]), and more than one nucleation mechanism may be operative, the applicable mechanism of nucleation continues to be debated. Nevertheless, there appears to be a difference in the nucleation processes associated with graphitization in the weld HAZ and the more recently documented base metal phenomenon attributed to plastic strain.

Weld HAZ Graphite Nucleation. In this case, graphite nucleation is believed to primarily occur during the welding thermal cycle at a base metal location experiencing peak temperatures in the cycle that are slightly above the lower critical Ac_1 temperature (≈1350 °F or 730 °C). Graphite nucleation probably occurs by the transformation of cementite (Fe_3C) to iron (Fe) and/or the transformation of the higher-C iron carbide, χ-carbide, to cementite.[14] The primary driving force for the transformation is the carbon activity gradient between the austenite (with high C solubility) formed above Ac_1 and the matrix ferrite (low C solubility), which results in a supersaturation of C on cooling. The supersaturation of C may also occur at sites rich in Al and/or Si by the oxidation of these elements.[15] Such a mechanism of supersaturation is probably responsible for the reported increased graphitization susceptibility with increasing Al and Si. However, this oxide formation mechanism for C supersaturation is likely to nucleate graphite only in the primary graphitization (solidification) phase, not in the weld thermal cycle, and is therefore expected to aggravate age-related, secondary graphitization only by providing the pre-existing nuclei to facilitate graphite growth.

One requirement for any location to qualify as a potential nucleating site is the presence of transformation volume change-accommodating defects in the form of vacancies and dislocations, high densities of which are associated with grain boundaries,[16] inclusions,[12] strain-induced defect clusters at various locations,[16] or all of the above at a single location. The effect of strain (deformation) is probably insignificant in the case of weld HAZ graphitization, but can influence base metal graphitization, as discussed below. Given the relatively small critical nucleus size and the numerous nucleating sites available during the solidification of typical iron and steel, it is likely that graphitization is controlled more by factors influencing graphite growth, rather than graphite nucleation. This is supported to some extent by more recent observations that Al and Si do not appear to have a significant effect on graphitization in the longer term (>30 years).[9,17] In the case of weld HAZ graphitization, the C supersaturation effect caused by the formation of austenite provides a significant driver for both nucleation and subsequent growth.

Base Metal Graphite Nucleation. Severe graphitization in the weld-unaffected base metal of carbon and low alloy steel in elevated-temperature service has only recently been observed.[10,11] The phenomenon, which has been suggested as being related to plastic strain,[11] has not been studied in as much detail as has been the weld HAZ graphitization process. Nevertheless, the potential effect of accumulated plastic strain on enhancing the susceptibility of iron and steel to graphite nucleation and growth was published nearly 30 years ago.[16,18] Harris *et al.*[16] suggested that the Cottrell atmosphere associated with dislocations may be instrumental in graphite nucleation. At a minimum, the high density of dislocations at slip obstacles generated as a result of plastic strain can provide the accommodation for the volume changes associated with graphite formation.[12] Niedzwiedz *et al.*[18] have even suggested that strain aging may produce C supersaturation at locations of high defect concentrations such as a grain boundary. In addition to this, the graphitizing effect of inclusions that may be present (see the C supersaturating effect described above for weld HAZ graphitization) is enhanced by the accumulation of strain-produced dislocations at the inclusion-matrix interface (inclusions behave as slip obstacles).

Graphite Growth

While there appear to be reasonable explanations for, and qualitative descriptions of, the graphite nucleation phase, the quantitatively useful time-temperature data on the nucleation phase is relatively limited. The graphitization prediction technique offered here has, therefore, been developed entirely from estimation of the kinetics of graphite growth (progression), assuming the pre-existence of graphite nuclei. This assumption appears reasonable, given the numerous potential graphite nucleating sites and apparent submicroscopic critical nucleus size in carbon and low alloy steels.

The progression of graphitization is essentially controlled by the growth of individual graphite particles or nodules. The specific rate at which such growth occurs is controlled largely by the rate at which free C can be produced at, or transported to, the graphite particle. A key issue associated with predicting graphitization in operating power (or other) plant steel components is the estimation of the graphitization progression rate, which is directly related to the graphite particle growth rate.

The kinetics of graphitization progression or growth have been described by a sigmoidal (S-shaped) growth function or curve (*e.g.*, Ref 15):

$$y = 1 - \exp(-Bt^n) \qquad \text{(Eq 1)}$$

where

y = the completed transformation fraction,
t = exposure time, and
B and n = constants.

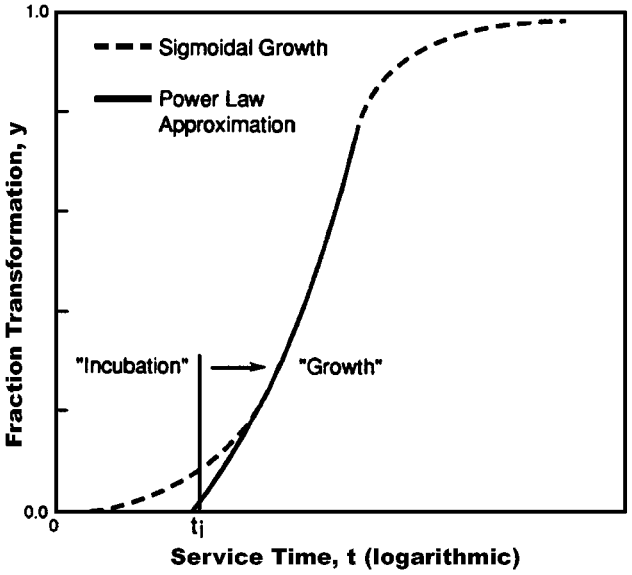

Fig. 3 Schematic of graphite growth kinetics; dashed line shows actual sigmoidal growth and solid line represents power-law approximation to major portion of the curve. Note the definition of an incubation period as a consequence of the approximation

The form of Eq. 1 does not provide a means of quantifying the thermal activation involved in the growth process, nor does it enable easy comparison between the growth rates in different situations (material and exposure temperature). Review of the published sigmoidal growth curve data (graphite percent versus logarithmic time) for C and C-Mo steels[15,19,20] shows that a major portion of the growth curve following the initial S bend can be approximated by a power dependence on exposure time; *i.e.*,

$$y = Ct_g^m \qquad \text{(Eq 2)}$$

where

m = a constant;

t_g = the exposure time following "incubation," = $t - t_i$, where t_i is the incubation time (see below); and

C = a temperature-dependent constant.

Figure 3 is a schematic of a typical sigmoidal growth curve (dashed line) showing the approximation (solid line). Also shown is a graphical definition of incubation, t_i. The physical significance of t_i is not known, but it facilitates the fitting of Eq. 2 to the observations. The temperature-dependent constant, C, may be replaced by an Arrhenius term describing a rate-controlling thermally activated process, so that Eq. 2, in the most general form, becomes

$$y = A \exp(-Q'/RT)\, t_g^m \qquad \text{(Eq 3)}$$

where

A = a constant,

T = the exposure temperature in absolute units,

R = the universal gas constants, and

$Q' \propto Q$, where Q is the activation energy for the controlling process Q' is expected to be equal to $3Q/2$ for radial diffusion-controlled growth.

Eq. 3 will henceforth be used to describe the kinetics of graphite growth beyond incubation.

Time Dependence of Graphitization. Fujihira [21] has demonstrated from laboratory tests that, at a given aging temperature, the radial growth of individual graphite particles of nodules is parabolic in time; *i.e.*, the particle radius, $r \propto t_g^{0.5}$. This proportionally implies that the graphite volumetric growth (proportional to r^3) and, therefore, the fraction transformation, y, is dependent on $t_g^{1.5}$ ($m = 1.5$ in Eq. 3). An analysis of the published experimental growth curves of Tanaka and Fujihira[20] on as-quenched nickel steel (2% Ni, 1.2% Si, and 0.24% C) and Niedzwiedz *et al.*[18] on as-quenched carbon steel (0.3% Al and 0.8% C) shows good agreement with this predicted exponent. It is important to note that the dependence of m on the quenching temperature (temperature from which quenching was carried out) was observed by Tanaka and Fujihira[20] to be negligible over a large range of quenching temperatures above Ac_1.

It appears from review of the literature on "laboratory" graphite coarsening that, for the carbon and low alloy steels of interest, while the incubation period and actual graphite growth rate may vary as a function of the material chemistry, microstructure, and initial heat-treatment condition (primarily through variation in the constant C of Eq (2), the time dependence (power, m) of the growth rate does not depend on these variables.

Temperature Dependence of Graphitization. Numerous attempts have been made to determine what process controls the growth rate of graphite particles/nodules (*e.g.*, 16, 21, and 22). The approach taken is consistent with the classic one used for time-dependent thermally activated processes (creep, carbide coarsening, *etc.*) wherein the rate-controlling process is established through measurement of the activation energy, Q (see Eq. 3). The following table summarizes the published activation energies for selected diffusing species and the activation energy values for graphitization as published or derived from published data.

The table illustrates the variability in the observed and derived activation energy values associated with graphitization and compares these values with the published activation energies for diffusion of pertinent species in α-Fe (ferrite). The apparent activation energy varies from a low of approximately 20 kcal/mole (84 kJ/mole) for the as-quenched Ni steel[20] to a high of 59 kcal/mole (251 kJ/mole) for the ductile cast iron with a 1% Mo addition.[22] Rundman and Rouns[22] have shown the effect of Mo in increasing the activation energy and reducing the graphite growth rate in case of the ductile irons. The increase in activation energy with Mo additions can be explained on the basis of the improved stability of the Mo carbides over the metastable iron carbides (Fe_3C, for example). Indeed, the apparent effectiveness of Cr additions to steel in reducing or eliminating the possibility of graphitization is as a result of even greater stability of the Cr carbides than is seen with the Mo carbides. Obviously, changes in the apparent activation energy and rate of graphitization can be made by alloy additions. The following key observations are summarized in relation to the observed activation energies.

Table 1 Activation energy, *Q* as published or derived from published data

Material	Process	Activation energy, *Q* kcal/mol (kJ/mol)	Reference Derivation
α-Fe (ferrite)	Diffusion of C in α-Fe	20 (84)	23/as-published
α-Fe (ferrite)	(Self/vacancy) Grain boundary or core diffusion	41 (174)	24/as-published
α-Fe (ferrite)	(Self/vacancy) lattice diffusion	60 (251)	25/as-published
Ni steel quenched from 1400 °F (2% Ni, 1.2% Si, 0.24% C)	Graphite nodule growth	20.5 (86)	20/derived from Fig. 3 [18] at = 50 h
Ni steel normalized (2% Ni, 1.2% Si, 0.24% C)	Graphite nodule growth	34.5 (145)	20/derived from Fig. 1 of [20] at t = 50 h
C-0.5 Mo steel	Graphitization to 50%	33.6 (141)	1/derived by Eq. 3
Ductile iron (3.5% C)	Graphitization to 50%	30 (126)	22/as-published
Ductile iron with Mo (3.5% C, 1% Mo)	Graphitization to 50%	59 (248)	22/as-published

- For the entire range of carbon steels (without Cr or Mo additions) on which graphitization data are available, there appears to be little effect of chemistry, including the carbon content, on the activation energy. This is consistent with the minimal effect of Al and Si (believed to be graphitizers) in the long term,[9,17] and the inference made earlier that Al and Si probably influence nucleation with little effect on growth in the long term.
- Fujihira's results[21] show the effect of quenching from 1400 °F (760 °C), or just above Ac_1. The graphite growth activation energy in such a case is reduced considerably from the as-normalized condition and approaches the activation energy for diffusion of C in α-Fe. This condition, with the lowest apparent activation energy and generally fastest graphite growth rate, is typical of that associated with the relatively well-known weld HAZ graphitization phenomenon.
- Fujihira also showed[21] that the graphite growth activation energy in as-normalized steel is closer to that for vacancy/self-diffusion along grain boundaries or dislocation cores than for the diffusion of C in α-Fe. He also showed that cold work can reduce the "as-normalized" activation energy in a direction toward the low end, as-quenched or weld HAZ graphitization process value.

Thus, a conservative prediction of graphitization in the case of weld HAZs of C, C-Si, and C-Mo steels may be made as a specific case of Eq 3, using a value for Q' as equal to the minimum activation energy for diffusion of C in α-Fe.

Currently, there exists insufficient data to quantitatively establish the effect of cold work or plastic strain on graphite growth. Nevertheless, the activation energy for grain boundary or core diffusion of 41 kcal/mole may be considered a lower bound for prediction of base metal graphitization in cases of plastic strain. Further, the 74% cold-rolled Ni steel graphitization activation energy was observed by Fujihira[21] to be somewhere between that for the as-quenched and the as-normalized steel. Thus, a preliminary, and believed to be conservative, growth rate equation for prestrained C and C-Mo steel base metal graphitization in elevated-temperature service is offered as a specific case of Eq. 3, using a value for Q' as equal to the activation energy for grain boundary or core diffusion (=41 kcal/mole).

Predicting and Quantifying Graphitization in Service

The available published field experience was reviewed to estimate the incubation period, t_i, preceding the apparent growth phase, and to quantify the kinetics of graphite growth (progression) in terms of Eq 3.

Analysis of Field Experience

The following sets of field data have been reviewed and analyzed:

- for C steel (A70, A285 plate; A106 pipe): Ref 2, 7, 9, and 26;
- for C-Si steel plate (A201): Ref 7 and 26, and
- for C-Mo steel (A206): Ref 2, 6, 7, 9, 26, and 27.

Nearly all of the data reviewed were for weld-related graphitization. Inferences made from the results of the review for prediction of graphitization in non-weld-related situations are discussed following the analysis.

All of the available data are in a form wherein the extent (degree) of graphitization is reported in qualitative fashion (*e.g.*, none, slight, moderate, or severe). The reported level of graphitization has been converted to a classification system based on the earliest classification procedure for degree of graphitization.[27] The degree of graphitization, G, is represented by 0 (no observed graphitization), 1 (very slight), 2 (slight), 3 (moderate), 4 (heavy), and 5 (severe, near or at failure). Based on the graphite volume percent growth curve and corresponding microstructures (apparent degree of graphitization) published by Samuels,[19] these classes were then converted to an equivalent "fraction of transformation complete," y, by

$$y = 0.2G \qquad \text{(Eq 4)}$$

The fitting of Eq 3 to the field data required first an estimation of the incubation period, t_i, as defined in Fig. 3. Review of Samuels'[19] and Tanaka and Fujihira's[20] sigmoidal growth curves showed that the incubation period varied from 0.5 to 0.7 times the time to reach a graphitization degree, G = 1, or a

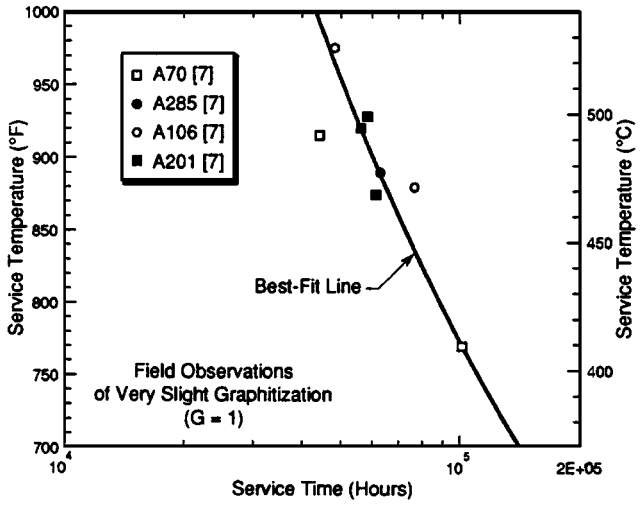

Fig. 4 Field data on "very slight" graphitization ($G = 1$) and the best-fit curve used to estimate the incubation period function

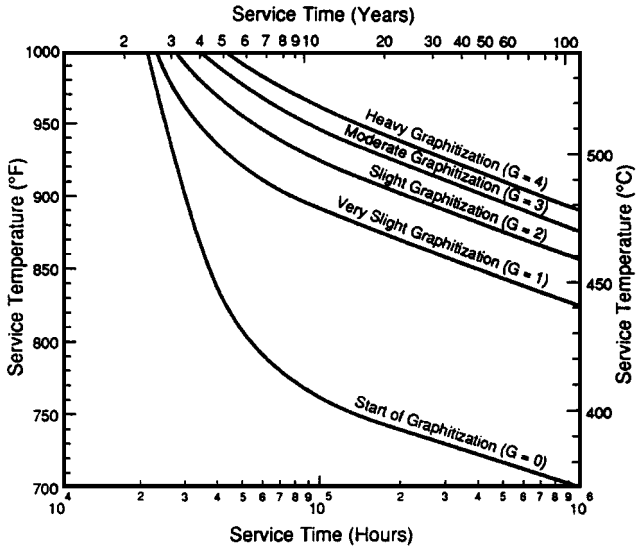

Fig. 5 Graphical summary of the best-fit TTT curves for various weld HAZ graphitization levels developed from Eq 7

transformation fraction, $y = 0.2$ (20% graphitization complete). The curve-fitting procedure used here included estimation of an approximate incubation period, $t_i = 0.5t_{0.2}$, where $t_{0.2}$ is the predicted time to reach $y = 0.2$ or $G = 1$. While there were several field observations of no graphitization ($G = 0$), these could not be easily used to estimate the incubation period.

Figure 4 shows the apparent time-temperature-transformation (TTT) behavior of the $y = 0.2$ ($G = 1$) data analyzed for C and C-Si steel. Also shown is the best-fit regression line (regression coefficient = 0.89) through the data:

$$t_{0.2} = 452.49 \exp (3693/T)$$

where $t_{0.2}$ is in hours and T in ° Kelvin (Eq 5)

It is important to note that the data (11 data points) were on a wide range of C steels, A70 and A285 plate steel and A106 pipe steel, and a C-Si steel, A201. In addition, the Al content varied from as low as 0.003% to as much as 0.150%. The reasonably good fit to the data supports the earlier conclusion that, in typical service, the effect of Al and Si is not significant.

From Eq 5, the incubation period is then estimated as $0.5t_{0.2}$, or

$$t_i = 226.25 \exp (3693/T) \quad \text{(Eq 6)}$$

Eq 6 was then used to estimate the "growth" period, t_g, for each data point analyzed, using $t_g = t - t_i$, where t is the reported exposure period. All the data were subsequently used for the Eq 3 curve fit.

The data used for the fit included.

- For C steel, 34 data points from Ref 7, 1 from Ref 9, and 1 from Ref 2.
- For C-Mo steel (A206): one data point each from Ref 6, 9, and 27. The available graphitization data on C-Mo steel was too limited to establish the effect of Mo additions. However, it should be noted that the limited C-Mo steel data show fair agreement with the C and C-Si steel behavior.

The data at a graphitization level $G \geq 2$ showed significant scatter. Uncertainties in temperature and interpretation of graphitization level are likely sources of scatter. Nevertheless, the curve of Eq 3 was fit to all the $G \geq 1$ data by regression, permitting the constants, A and m, to vary, and assuming a value of 20 kcal·K for Q'/R. This assumption for Q'/R translates to a value of approximately 40 kcal/mole for Q', or 26 kcal/mole for the activation energy, Q, if $Q' = 3Q/2$. The assumption on Q' became essential since the nature of the scatter in the data forces the regression using Q' as a variable to tend toward unrealistically low values of Q' and m. A fixed value of Q' therefore was selected such that the regression-based fit would result in $m \geq 0.5$ and produce the minimum sum of squares of the difference between the actual and predicted y values. The following best-fit values for the constants in Eq 3 were obtained:

$A = 2.07 \times 10^8$ and $m = 0.53$ for $Q'/R = 20{,}000$ K; *i.e.*, for weld HAZ graphitization:

$$y = 2.07 \times 10^8 \exp (-20{,}0000/T)\, t_g^{0.53} \quad \text{(Eq 7)}$$

where y is the fraction of transformation complete, T is the exposure temperature in K, and t_g is the growth period following the incubation period, t_i, in hours estimated by Eq 6.

The exponent m (=0.53) is significantly lower than the anticipated value of 1.5 based on the expected parabolic linear growth kinetics.[21] Reasonable adjustments to Q' did not produce a sufficient increase in the best-fit m value to eliminate this disagreement. This discrepancy between the field and theoretical/laboratory power dependence remains an issue.

Figure 5 is a graphical representation of the best-estimate TTT curves obtained for various transformation (degree of graphitization) levels using Eq 7. The curves represent approximate best estimates and may be nonconservative in some cases.

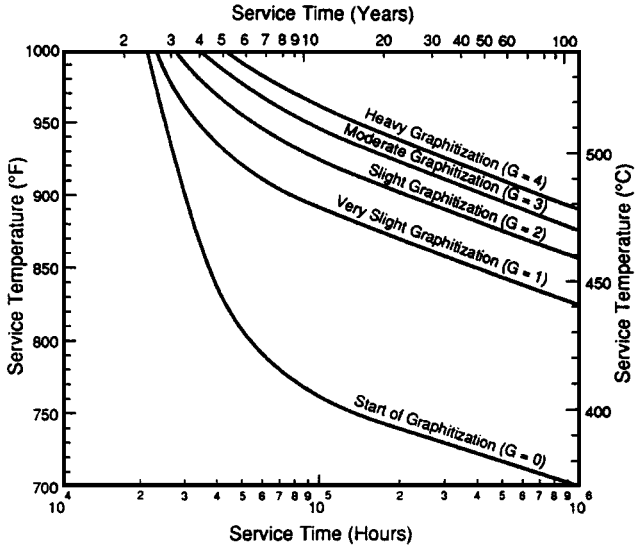

Fig. 5 Graphical summary of the best-fit TTT curves for various weld HAZ graphitization levels developed from Eq 7

Nevertheless, they may be used as first-approximation guidelines for predicting weld HAZ graphitization in C, C-Si, and C-Mo steels.

Several conclusions can be made from the results of the field data analysis:

- Despite a significant variation in deoxidizer and trace element content (for example, $0.003\% \leq Al \leq 0.150\%$), it is interesting to note that, for all the C and C-Si steels, the $y = 0.2$ ($G = 1$) curve represents a very good fit to the data (Fig. 4). This supports the literature-review-based inference that Al and Si do not appear to have a significant effect on the graphitization process as is widely believed.
- As a first approximation, the TTT curves of Fig. 5 may be used to predict graphitization in weld HAZs of C, C-Si, and C-Mo steels in service. However, for graphitization levels exceeding $G = 1$ ("very slight"), the scatter in the field data is significant, and the uncertainty in the pertinent TTT curve predictions should be recognized.
- The TTT curves of Fig. 5 are offered for application only to weld HAZ graphitization in C, C-Si, and C-Mo steels. The more recent, base metal graphitization phenomenon is probably better described by separate kinetics that may be developed as field experience becomes available. Currently, however, it is believed that the weld HAZ graphitization curves may be conservatively used for application to the base metal problem.

Effect of Al and Si on Graphitization

It has, for some time, been widely believed that graphitization is significantly influenced by the presence of the deoxidizing elements, Al and Si, added to steel (*e.g.*, Ref 19). Several mechanisms for the role of deoxidizers on enhancing graphitization have been proposed. These have included the possibility of the Al and Si oxides providing graphite nucleation sites,[19] the formation of Al and Si oxides resulting in the liberation of C and an increase in C concentration around these oxides,[15] and the propensity for Al to form nitrides, thereby reducing the free nitrogen and increasing the interstitial carbon available for graphitization.[11] However, as explained in the preceding sections, review of the published literature[9,17] and the analysis of the available field experience on the graphitization of C and C-Si steels performed here shows that the effect of Al and Si on graphitization in the long term is negligible. The conclusion is consistent with the inference made earlier that graphitization is probably controlled more by the rate of graphite growth than by graphite nucleation, and that while Al and Si can enhance nucleation and near-term graphite growth, they can be expected to have little effect under longer-term graphitization conditions typical of most applications.

Effect of Graphitization on Service Life

Given the ability to roughly predict the extent of graphitization, key issues are the *in-situ* determination of the graphitized condition of the operating component and the effect of graphitization on the remaining life of the component. The TTT curves provide a means of prioritizing components and component locations for inspection of graphitization. The prioritization is facilitated by newly available nondestructive methods for estimating fossil plant component operating temperatures (*e.g.*, Ref 28). It is likely that, as more accurate operating temperature estimates are made, graphitization will become more accurately predictable.

The outer surface condition of an operating component can be easily evaluated for graphitization by metallographic field replication procedures (*e.g.*, Ref 29) currently used to characterize various forms of microstructural damage, including creep-related damage. The estimation of observed graphitization on the remaining life of the component, however, is a more complex matter. This is because severe localized graphitization not only reduces the stress rupture life of the material, but can also facilitate time-dependent crack growth and premature catastrophic fracture by a fracture toughness reduction (embrittlement). While there is limited data on the effect of graphitization on stress rupture life,[2] there is little or no quantitatively useful information on how graphite influences crack growth and fracture toughness. Such mechanical properties at localized regions of the component showing surface graphitization can now be characterized by application of a virtually nondestructive, surface material sampling approach[30] routinely used for turbine steel embrittlement characterization (*e.g.*, Ref 31). It should be noted that, based on review of the published experience, the application of a possible *in-situ* reheat treatment for reversing graphitization at the lower levels ($G \leq 3$) appears to be impractical and of limited life extension value.

Stress Rupture Life. Review of Creamer's graphitization and as-graphitized steel stress rupture data for A201 carbon steel ex-service plate[2] provided some preliminary insight into the effect of graphitization on rupture life. The two cases gave an interesting comparison.

- Steel A: A201 Grade A, reported to be heavily graphitized in the form of random nodules after 30 years at 900 to 925 °F (482 to 496 °C); y was estimated to be 0.6 to 0.8 per Eq 7.
- Steel D: A201 Grade B, reported to have no graphitization,

but to have nearly fully spheroidized after 18 years at 950 °F (510 °C).

It was interesting to note that, in each case, the laboratory stress rupture data indicated an approximate rupture life fraction consumed of 0.7; *i.e.*, it did not seem to matter whether the material was graphitized or spheroidized. The consumed life fraction was estimated, from Fig. 5 and 11 of Ref 2, by using a design stress estimated from the ASME Code curve at the reported temperature and by comparing the "laboratory rupture" Larson-Miller parameter value with the mean "ASTM data" Larson-Miller parameter value (the ASTM data are assumed to represent "new" material). The results suggest that the random nodule graphitization form has an effect on rupture life that is comparable with the effect of spheroidization on rupture life. The better-known spheroidization effects on material rupture life (*e.g.*, Ref 32) therefore may be used to approximate the effect of random nodule graphitization on material rupture life. Thus, where a random nodule graphite morphology is identified by, for example, surface replication, a life prediction may be made on the basis of stress-rupture life, as described above. On the other hand, the discovery of the material-embrittling, planar graphite form, whether in weld HAZ or base metal, would require consideration of a flaw tolerance approach to assessing future component integrity, as summarized below.

Crack Growth and Embrittlement. Establishing component flaw tolerance under graphitizing conditions requires, among other things, the material subcritical (creep) and critical (fracture toughness) crack growth properties. This is especially important when the graphite morphology includes a localized, planar form. The material fracture properties as a function of graphitization condition have yet to be developed. The early bend test results of Thielsch *et al.*[27,33] while providing a means of characterizing fracture behavior as a function of graphitization, do not help a quantitative assessment of flaw tolerance and remaining life by fracture mechanics methods. While no immediate solutions are available to the problem of predicting the subcritical growth of a crack in graphitized material, techniques are available to measure the material fracture toughness in order to safeguard against catastrophic component failure by unstable growth of a critical crack. The material fracture toughness may be measured on a component- and location-specific basis by application of recently developed relatively nondestructive miniature sampling and testing methods that are currently being applied to operating fossil power plant components.[31,34] Measurement of fracture toughness then permits quantifying the tolerable size of flaw for establishing the risk of component failure and for developing an appropriate component inspection and maintenance program.

Conclusions

The review and analysis of published literature and laboratory and field data on the graphitization of steels produced the following conclusions relevant to elevated-temperature fossil plant steel components.

- The TTT curves for approximate prediction of graphitization in weld HAZs of C, C-Si, and C-Mo steels have been developed from published field data. The prediction has also been offered as a preliminary prediction for base metal (non-weld-related) graphitization. It is important to note that the TTT curves are best-estimate approximations and can prove nonconservative in some cases. Nevertheless, the curves provide a valuable means of helping prioritize components and component locations for inspecting for graphitization.
- The Al, Si, and trace elements appear to have a negligible influence on the long-term graphitization of C steel. Similarly, the limited data on material with Mo additions to 0.5% could not be shown to have a major effect on reducing the graphitization of C steel.
- The limited ex-service materials stress rupture data suggest that remaining life predictions in cases where component life is stress rupture controlled (*i.e.*, in cases where graphitization occurs in random nodule fashion) may be made by treating graphitization as identical to spheroidization. Structural reliability analyses in cases of localized weld HAZ or base metal, planar graphitization require some estimation of the subcritical and critical material crack growth properties for the graphitized zone.
- Since the effect of graphitization on crack growth behavior is not known, it is recommended that component-specific sampling and miniature specimen test approaches currently being used for material toughness evaluations be used to quantify component flaw tolerance in cases where graphitization appears to be localized and of concern.

Acknowledgment

The Electric Power Research Institute supported this research effort under Project No. RP2426-53. D. Dedhia, Failure Analysis Associates, Inc., is acknowledged for assistance with the data analysis and curve fitting. R. Hellner, Public Service Co. (PSC) of Colorado, is thanked for sharing PSC's recent experience on non-weld-related graphitization in boiler tubes.

References

1. *ASM Metals Handbook*, 10th ed., vol. 1, *Properties and Selection: Irons, Steels and High-Performance Alloys*, ASM International, Materials Park, OH, 1990, p. 644.
2. E.L. Creamer: *Evaluation of Materials in Process Equipment after Long Term Service in the Petroleum Industry*, ASME MPC-12, A.R. Ciuffreda, ed., ASME, New York, NY, 1980, pp. 13-21.
3. R.W. Emerson: *Trans. ASME*, 1944, vol. 66, pp. 5-15.
4. W.G. Conant and W.A. Reich: "Graphitization Studies of Materials for High-Temperature Service in Steam Plants," paper presented at the *ASME Annual Meeting*, New York, NY, 1946.
5. S.H. Weaver: *Trans. ASME*, 1946, vol. 68, p. 631.
6. J.B. Nuchols and J.R. McGuffey: *Mech. Eng.*, 1959, vol. 81 (5), pp. 43-45.
7. J.G. Wilson: *Graphitization of Steel in Petroleum Refining Equipment and The Effect of Graphitization of Steel on Stress-Rupture Properties*, Welding Research Council Bulletin No. 32, Welding Research Council, New York, NY, 1957.
8. I.A. Rohrig: *Williamsburg Station Accident Investigation*, Dec. 1977.
9. W.R. Pavlichko and A. Solomon: *Microstr. Sci.*, 1980, vol. 8, pp. 231-45.
10. R.D. Port: *Corrosion 89*, Apr. 1989, NACE, Houston, TX, 1989.
11. R.D. Port, W.C. Mack, and J. Hainsworth: *Proc. 1st Int. Conf. on Heat-Resistant Materials*, ASM International, OH, 1991, pp. 587-94.

12. A.A. Baranov and K.P. Bumin: *Russ. Castings Prod.*, 1964, vol. 7, pp. 317-19.
13. F.K. Tkachenko: *Russ. Castings Prod.*, 1962, vol. 5, pp. 235-36.
14. M. Okada: *Trans. Jpn. Inst. Met.*, 1982, vol. 23 (7), pp. 353-59.
15. A. Rosen and A. Taub: *Mem. Sci. Rev. Metall.*, 1961, vol. 58, p. 957.
16. J. Harris, J. Whiteman, and A. Quarrell: *Trans. AIME*, 1965, vol. 233, p. 168.
17. Y.M. Gofman and G.G. Vinokurova: *Therm. Eng.*, 1988, vol. 35 (7), pp. 392-94.
18. S. Niedzwiedz, A. Taub, and B.Z. Weiss: *Isr. J. Technol.*, 1966, vol. 4 (4), pp. 233-42.
19. L.E. Samuels: *Optical Microscopy of Carbon Steels*, ASM, Metals Park, OH, 1980, p. 245.
20. R. Tanaka and A. Fujihira: *J. Jpn. Inst. Met.*, 1966, vol. 30 (3), pp. 279-84.
21. A. Fujihira: *J. Jpn. Inst. Mets.*, 1980, vol. 44 (1), pp. 6-15.
22. K.B. Rundman and T.N. Rouns: *Trans. AFS*, 1982, vol. 82 (117), pp. 487-97.
23. C. Wert: *Phys. Rev.*, 1950, vol. 79, p. 601.
24. D.W. James and G.M. Leak: *Phil Mag.*, 1965, vol. 12, p. 491.
25. F.S. Buffington, I.D. Bakalar, and M. Cohen: *Acta Metall.*, 1961, vol. 9, p. 434.
26. W.B. Bedesem: *Evaluation of Materials in Process Equipment after Long Term Service in the Petroleum Industry*, ASME MPC-12, A.R. Ciuffreda, ed., ASME, New York, NY, 1980, pp. 1-12.
27. H. Thielsch, E.M. Phillips, and E.R. Jerome, Jr.: *Welding J.*, 1955, vol. 34, Research Suppl., pp. 286s-294s.
28. R. Viswanathan, J.R. Foulds, and D.I. Roberts: *Proc. Int. Conf. on Life Assessment and Extension*, The Hague, June 1998, paper no. 1.6.2.
29. G. Kerzner, I. Sprung, and V. Zilberstein: *Mater. Eval.*, 1989, vol. 47 (9), pp. 1008-18.
30. J.D. Parker, A. McMinn, and J. Foulds: *PVP—Vol. 171, Life Assessment and Life Extension of Power Plant Components*, T.V. Narayanan *et al.*, ASME, New York, NY, 1989, Book No. H00486, pp. 223-30.
31. J.R. Foulds, C.W. Jewett, L.H. Bisbee, T.L. Gabel, and R. Viswanathan: *Proc. 1992 Int. Joint Power Generation Conf.*, ASME, PWR- vol. 18, Steam Turbine-Generator Developments for the Power Generation Industry, W.G. Steltz, ed., Book No. G00688, ASME, New York, 1992.
32. L.H. Toft and R.A. Marsden: *Conf. on Structural Processes in Creep*, JISI/JIM, London, 1963, p. 275.
33. H. Thielsch: *Defects and Failures in Pressure Vessels and Piping*, Reinhold Publishing Co., New York, NY, 1965, pp. 49-83.
34. "Small Punch Testing for Fracture Toughness Measurement," EPRI TR-105130, EPRI, Palo Alto, CA, 1995.